Role of Electronic Excitations in Ion Collisions with Carbon Nanostructures

Arkady V. Krasheninnikov,[1,2] Yoshiyuki Miyamoto,[3] and David Tománek[4]

[1]*Accelerator Laboratory, P.O. Box 43, FIN-00014 University of Helsinki, Finland*
[2]*Laboratory of Physics, Helsinki University of Technology, P.O. Box 1100, Helsinki 02015, Finland*
[3]*Nano Electronics Research Laboratories, NEC Corporation, 34 Miyukigaoka, Tsukuba, 305-8501, Japan*
[4]*Physics and Astronomy Department, Michigan State University, East Lansing, Michigan 48824-2320, USA*

(Received 7 February 2007; published 6 July 2007)

By combining *ab initio* time-dependent density functional calculations for electrons with molecular dynamics simulations for ions in real time, we investigate the microscopic mechanism of collisions between energetic protons and graphitic carbon nanostructures. We identify not only the amount of energy lost by the projectile, but also the electronic and ionic degrees of freedom of the target that accommodate this energy as a function of the impact parameter and projectile energy. Our results establish validity limits for the Born-Oppenheimer approximation and the threshold energy for defect formation in carbon nanostructures.

DOI: 10.1103/PhysRevLett.99.016104 PACS numbers: 81.07.De, 34.50.Bw, 61.80.Jh, 73.63.Fg

Interaction of energetic particles with nanostructures plays a fundamental role both in the field of ion beam irradiation and in nanoscience. Of basic interest are the microscopic mechanisms of defect formation and the related radiation hardness of carbon nanostructures, including nanotubes [1], in the outer space. Furthermore, there is a desire to understand and optimize ion beam irradiation as a means to modify mechanical [2], electronic [3,4], and magnetic [5,6] properties of nanostructured carbon. Interestingly, the extensive body of published results on ion stopping in solids [7–13] provides no microscopic information about the most basic questions, such as the amount of energy deposited into electronic and vibrational degrees of freedom of graphene or a carbon nanotube following the impact of an individual ion. Yet exactly this information is a critical input parameter in the Kinchin-Pease theory of defect production [14] and the prevalent semiclassical Ziegler-Biersack-Littmark (ZBL) theory of ion stopping [7].

Even though semiclassical methods, based on fits to experimental data, successfully reproduce radiation damage to solid samples as an average over many collisions, their extension to very thin targets [7] and nanostructures [15] has been shown as inadequate. In particular, the common separation of energy deposition during collisions into uncorrelated ''nuclear'' and ''electronic'' energy losses ignores the crucial role of electronic excitations in modifying the interaction between ions and eventually mediating formation of defects in nanostructures.

Here we combine time-dependent density functional (TDDFT) [16] calculations for electrons with molecular dynamics (MD) simulations for ions [17] in order to obtain microscopic insight into the role of electronic excitations during collisions between energetic ions and sp^2 bonded carbon nanostructures, including graphene sheets and single-wall nanotubes. By considering the dynamics of electrons and ions in real-time simulations at the *ab initio* level, we gain valuable insight into the deviation of the system dynamics from ground-state dynamics based on the Born-Oppenheimer (BO) approximation. Our results identify the amount of energy deposited into the target as a function of the ion energy and impact parameter and provide a bias-free insight into how this energy is distributed over the electronic and ionic degrees of freedom. We demonstrate quantitatively the growing role of electronic excitations with increasing ion impact energy and, as a side result, identify the threshold energy for monovacancy formation in graphene and nanotubes.

We chose hydrogen as a projectile due to the importance of electronic degrees of freedom during the impact of light ions and thus likely deviations from the adiabatic picture in collision processes. Graphene layers [18] and single-wall carbon nanotubes (SWNTs) [19] are interesting targets that exhibit a wide range of intriguing electronic properties, which can be modified by ion beam irradiation [2,3,20–23]. More significant is the need to reconcile the discrepancy between the modest proton irradiation dose of $\leq 10^{17}$ protons/cm^2 that was found sufficient to destroy SWNTs [22,24,25] and results based on the ZBL theory [7] that lie several orders of magnitude higher [26,27].

Unlike parametrized empirical theories of ion stopping [7,9], our *ab initio* simulations, performed using the FPSEID (first principles simulation tool for electron-ion dynamics) code [17], offer an unbiased microscopic insight into the projectile-target interaction, since TDDFT-MD treats electron and ion dynamics on the same footing in real time. Our approach explicitly takes into account the electronic structure of the target and thus discriminates among different carbon allotropes, including diamond and graphite. In this sense, it is superior to the ZBL approach [7] that characterizes the target only by atomic number and density [27], or model TDDFT simulations that represent the target by a uniform electron gas [28]. Since the systems of interest are well above zero temperature, the ionic motion is described

classically, with forces acting on the ions given by the density functional theory in the local density approximation (LDA) [29]. The electron-ion interaction is described using norm-conserving pseudopotentials [30], and the valence wave functions are expanded in a plane-wave basis with a kinetic energy cutoff of 40 Ry. This computationally demanding approach has proven very useful to describe photochemical processes [31] and to understand the damping mechanism of electronic excitations [32] in carbon nanotubes.

Our calculations were performed using periodic boundary conditions with large supercells. Graphene layers, separated by 10 Å, were represented by 7×7 supercells, containing 98 atoms, or by smaller 4×4 cells with 32 atoms. We found results for the larger supercell, sampled by 1 k point, to agree with those for the smaller supercell, sampled by 2 k points. Alternatively, we considered a superlattice of (3, 3) armchair SWNTs with 72 atoms per unit cell and 10 Å interwall separation, sampled at the Γ point only.

To elucidate the effect of electronic excitations in the dynamics, we compared our TDDFT-MD results to BO-MD simulations of systems, where electrons were artificially confined to the ground state. For the sake of convenience, we represented the Born-Oppenheimer total energy functional by the nonorthogonal DFT-based tight-binding (DFTB) method [33]. Among others, this method has successfully described the energetics of defect formation and migration in carbon nanotubes [34–36].

To better understand the difference between experimental [22,24,25] and theoretical data, we first studied the key quantity of radiation physics, namely, the threshold displacement energy of carbon atoms in a target exposed to energetic H atoms. The simulation setup is shown schematically in the inset of Fig. 1. For maximum energy transfer between projectile and recoil atom, we considered head-on collisions with zero impact parameter. The threshold energy for vacancy formation in a graphene monolayer turns out to be $E_{\text{init}}(\text{H}) = 84$ eV in TDDFT-MD and $E_{\text{init}}(\text{H}) = 80$ eV in BO-MD simulations, with ≈ 22 eV transferred to the recoil atom. This fair agreement between TDDFT-MD and BO-MD simulations suggests that the binary collision approach [7] is applicable in this regime. Our finding that electronic excitations play only a minor role in this energy range is plausible, since the H atom velocity of $v_{\text{init}}(\text{H}) \approx 1.2 \times 10^5$ m/s lies well below the Fermi velocity of graphitic carbon, $v_F(\text{graphite}) = 8 \times 10^5$ m/s.

Obviously, deviations from ground-state dynamics are expected at projectile velocities approaching or exceeding $v_F(\text{target})$. Electronic excitations are expected to matter most in noncentral collisions with impact outside the cross section of the closest target atom, where direct kinetic energy transfer is not important. The parallel requirement of a large electron density for maximum effect can be best satisfied in the bond region. In our simulations, we selected the point of impact in the C-C bond region, 0.25 Å from the closest carbon atom. The collision geometry and numerical results for the C recoil energy are summarized in Fig. 1.

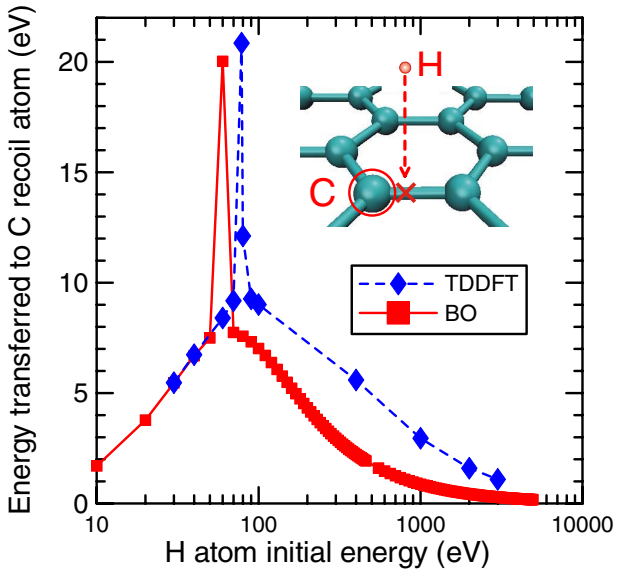

FIG. 1 (color online). Schematic geometry of a H projectile impacting normally onto a graphene target. The data points show the energy transferred to the recoil C atom, emphasized by a circle, as a function of the initial energy of the projectile, for an impact parameter of 0.25 Å along the C-C bond. Electronic excitations, considered in TDDFT and ignored in BO simulations, are important beyond ≈ 100 eV H impact energy.

As expected, the C recoil energy is small not only at small projectile energies, where energy transfer is limited, but also at large projectile energies, where the projectile-target interaction time is too short for energy transfer. An intriguing effect in our geometry is the sharp absorption peak near 80 eV, caused by a resonant double-collision with the closest two carbon atoms. We find the TDDFT-MD and BO-MD results to agree well up to $E_{\text{init}}(\text{H}) \approx 100$ eV, where the C atom recoil is maximized. At higher energies, TDDFT-MD and BO-MD results differ significantly due to the growing role of electronic excitations, which are ignored in BO-MD.

Next, we studied the accommodation of the energy transferred from the projectile into the individual degrees of freedom. Our results, which address this important question of radiation physics, are summarized in Fig. 2(a). The TDDFT-MD simulations not only reproduce the known trends, but also provide additional microscopic information. As inferred from the TDDFT-MD and BO-MD results for $E_{\text{init}}(\text{H}) > 100$ eV in Fig. 2(a), the energy transferred directly into the kinetic motion of all carbon atoms decreases with increasing projectile energy, similar to results in Fig. 1 for the C recoil atom. This simple trend, however, does not apply for the total energy transferred to the target, defined by the difference between the initial and the final kinetic energy of the H atom and shown by the solid lines in Fig. 2(a). Whereas BO-MD predictions for the total and the kinetic energy transfer are nearly indistinguishable,

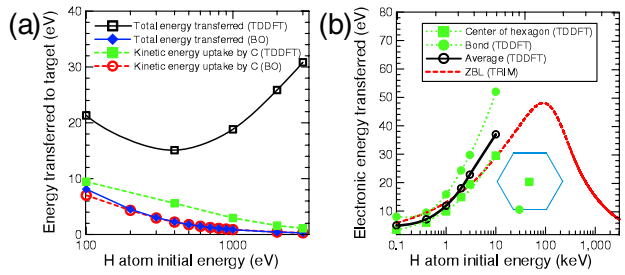

FIG. 2 (color online). Energy transferred to the graphene target following the impact of an energetic H atom for the impact geometry used in Fig. 1. (a) TDDFT-MD and BO-MD results for the total energy transferred to the target, shown by the solid lines, are compared to the kinetic energy uptake by the carbon atoms in the target, given by the dashed lines. (b) Energy transferred into the electronic degrees of freedom only. TDDFT-MD simulation results for impacts in the center of the hexagon and in the C-C bond with an impact parameters of 0.25 Å are given by the dotted lines. An estimated average over the surface, shown by the solid line, is compared to ZBL results of the semiempirical code TRIM [27], shown by the dashed line.

TDDFT-MD simulations suggest a qualitatively new trend, namely, an increase in the total transferred energy above H impact energy of ≈ 400 eV. This trend reversal, also observed in experiments, cannot be explained by BO-MD simulations and thus necessarily involves electronic excitations as an important effect.

Next, we wish to obtain additional information about the fraction of the total energy transferred into the electronic degrees of freedom. We focus on the interesting energy range $E_{\mathrm{init}}(\mathrm{H}) \gtrsim 0.4$ keV where, according to Fig. 2(a), electronic effects play an important role. This information can only be provided by TDDFT-MD simulations and is discussed in Fig. 2(b). Predictions of the semiempirical code TRIM [27], representing experimental expectations averaged over bulk graphitic targets, suggest a significant energy uptake of up to 50 eV, which is ignored in BO-MD simulations.

We limit our TDDFT-MD simulations to two representative trajectories. Further limitation on the energy range is imposed by the cutoff energy of our plane-wave basis. Our TDDFT-MD results for the entire system in Fig. 2(b), obtained by subtracting the kinetic energy of the H and C atoms from the total energy, appear to agree with experimentally expected electronic excitations in the target, represented by the TRIM simulations. The lower amount of electronic energy transferred for H passing through the hexagon center reflects the lower charge density at this point of impact. The solid curve in Fig. 2(b) is an estimated average across the target.

Our computational approach also correctly describes the case of grazing incidence, with the projectile trajectory parallel to the surface, where energy is transferred to the target by exciting plasmon modes. Unfortunately, it is fundamentally impossible to separate electronic excitations in the target from those in the projectile in TDDFT-MD simulations. The TDDFT-MD curves in Fig. 2(b) provide only an upper estimate for the electronic energy deposited in the target, since they also contain electronic excitations in the projectile, which may be affected by charge transfer to the target. In general, trajectories obtained by TDDFT-MD simulations were consistent with previously published BO-MD results [35], suggesting that the recoil C atom is either sputtered away from the system, or readsorbs and slides along the surface to a stop. If its final distance from the vacancy exceeds ≈ 3 Å, an immediate adatom-vacancy recombination is prevented.

Based on an analysis of the electron density and the electronic eigenvalue spectra, about 5–10 eV of the electronic excitation energy of the system can be attributed to the H projectile for relevant energies $E_{\mathrm{init}}(\mathrm{H}) \gtrsim 1$ keV. To describe electronic excitations in the target would require shifting the TDDFT-MD data in Fig. 2(b) downwards by this amount, thus further improving overall agreement with observed data. Curiously, the arising moderate disagreement between TDDFT-MD and TRIM results in the lower impact energy range $E_{\mathrm{init}}(H) \approx 0.1$ keV also correctly reproduces the fact that the TRIM parametrization overestimates the observed energy deposition in this energy range, thus providing further justification for the adequacy of our TDDFT-MD approach.

More detailed information about the electronic excitations in the projectile can be obtained by inspecting the time evolution of Kohn-Sham eigenvalue spectra during the collision, shown in Fig. 3. Closer inspection of these results suggests that the most prominent changes are associated with the excitation of the H1s level by few eV following the impact, whereas changes in the remaining spectrum are small. Additional results for the kinetic-energy-density evolution in the target furthermore suggest that the impacting H atom triggers a shock wave-type plasmon, which propagates radially from the point of impact with approximately the Fermi velocity of the target.

To estimate the role of target morphology in the collision process, we compared our graphene results to those for carbon nanotubes. Especially in the narrow (3,3) nanotube,

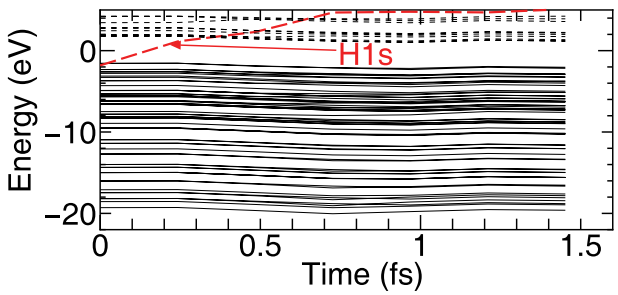

FIG. 3 (color online). Time evolution of the Kohn-Sham energy eigenvalues during the collision of a H atom with graphene. The normal impact of the H atom with an initial kinetic energy of 3 keV occurred at the center of a hexagon. After the collision, the H atom lost 20 eV of its initial kinetic energy.

which is barely stable, strain is expected to reduce the threshold energy for defect formation [36]. The simulation trajectories were constructed such that the H atom entered the nanotube through the center of a hexagon and left after colliding with a C atom at the other side. We indeed find a significant lowering of the threshold energy from 84 eV in graphene to 65 eV in nanotubes in TDDFT-MD and from 80 eV to 55 eV in BO-MD simulations. Here, we should also point out the important fact that, unlike in graphene, a collision with a nanotube involves a double collision with the front and the rear face. Electronic excitations, triggered at the first collision, affect the outcome of the second collision with the nanotube due to its quasi-one-dimensional tubular structure by slowing down the dissipation of the energy transferred from the projectile. This is a likely reason for the lower stability of nanotubes in comparison with graphitic systems even at very high impact energies, where head-on collisions are rare.

Since the interaction of a H atom with the target at the point of impact is rather insensitive to the initial charge state at low impact energies, we find very little difference between our simulations for neutral H and a proton as projectiles. We also should point out that ignoring core excitation processes, which would trigger a Coulomb explosion, does not limit the validity of our simulations, since Coulomb explosion has been excluded by previous work [12].

In conclusion, we combined *ab initio* time-dependent density functional calculations for electrons with molecular dynamics simulations for ions in real time to investigate the microscopic mechanism of collisions between energetic protons and graphitic carbon nanostructures. We identified not only the amount of energy loss of the projectile, but also the electronic and ionic degrees of freedom of the target that accommodate this energy as a function of the impact parameter and projectile energy. Our results generally agree with those of semiempirical calculations reproducing experimental data and establish validity limits for the Born-Oppenheimer approximation as well as the threshold energy for defect formation in carbon nanostructures.

We acknowledge fruitful discussions with K. Nordlund. A. K. was supported by the Center of Excellence Program of the Academy of Finland. Y. M. was supported by the Next Generation Super Computing Project, Nanoscience Program, MEXT, Japan. D. T. was supported by NSF-NIRT Grant No. ECS-0506309, NSF NSEC Grant No. 425826, and the Humboldt Foundation.

[1] S. Iijima, Nature (London) **354**, 56 (1991).
[2] A. Kis *et al.*, Nat. Mater. **3**, 153 (2004).
[3] G. Gómez-Navarro *et al.*, Nat. Mater. **4**, 534 (2005).
[4] H. Stahl, J. Appenzeller, R. Martel, P. Avouris, and B. Lengeler, Phys. Rev. Lett. **85**, 5186 (2000).
[5] P. Esquinazi *et al.*, Phys. Rev. Lett. **91**, 227201 (2003).
[6] S. Talapatra *et al.*, Phys. Rev. Lett. **95**, 097201 (2005).
[7] J. F. Ziegler, J. P. Biersack, and U. Littmark, *The Stopping and Range of Ions in Matter* (Pergamon, New York, 1985).
[8] *Atomic & Ion Collisions in Solids and at Surfaces: Theory, Simulation and Applications*, edited by R. Smith (Cambridge University Press, Cambridge, England, 1997).
[9] P. Sigmund, A. Fettouhi, and A. Schinner, Nucl. Instrum. Methods Phys. Res., Sect. B **209**, 19 (2003).
[10] P. M. Echenique, R. M. Nieminen, J. C. Ashley, and R. H. Ritchie, Phys. Rev. A **33**, 897 (1986).
[11] P. Stampfli, Nucl. Instrum. Methods Phys. Res., Sect. B **107**, 138 (1996).
[12] G. Schiwietz *et al.*, Nucl. Instrum. Methods Phys. Res., Sect. B **175–177**, 1 (2001).
[13] A. E. Volkov and V. A. Borodin, Nucl. Instrum. Methods Phys. Res., Sect. B **107**, 172 (1996).
[14] G. H. Kinchin and R. S. Pease, Rep. Prog. Phys. **18**, 1 (1955).
[15] T. Kunert and R. Schmidt, Phys. Rev. Lett. **86**, 5258 (2001).
[16] E. Runge and E. K. U. Gross, Phys. Rev. Lett. **52**, 997 (1984).
[17] O. Sugino and Y. Miyamoto, Phys. Rev. B **59**, 2579 (1999); **66**, 089901(E) (2002).
[18] K. S. Novoselov *et al.*, Nature (London) **438**, 197 (2005).
[19] *Carbon Nanotubes: Synthesis, Structure, Properties and Applications*, edited by M. S. Dresselhaus, G. Dresselhaus, and P. Avouris (Springer, New York, 2001).
[20] A. Hashimoto *et al.*, Nature (London) **430**, 870 (2004).
[21] L. Sun *et al.*, Science **312**, 1199 (2006).
[22] V. A. Basiuk *et al.*, Nano Lett. **2**, 789 (2002).
[23] B. Q. Wei, J. D'Arcy-Gall, P. M. Ajayan, and G. Ramanath, Appl. Phys. Lett. **83**, 3581 (2003).
[24] P. P. Neupane *et al.*, Appl. Phys. Lett. **86**, 221908 (2005).
[25] A. R. Adhikari *et al.*, Nucl. Instrum. Methods Phys. Res., Sect. B **245**, 431 (2006).
[26] Based on comparison with results obtained by the standard ZBL code TRIM [27].
[27] J. F. Ziegler and J. P. Biersack, computer code TRIM, 2003, http://www.srim.org.
[28] V. U. Nazarov, J. M. Pitarke, C. S. Kim, and Y. Takada, Phys. Rev. B **71**, 121106(R) (2005).
[29] J. P. Perdew and A. Zunger, Phys. Rev. B **23**, 5048 (1981); D. M. Ceperley and B. J. Alder, Phys. Rev. Lett. **45**, 566 (1980).
[30] N. Troullier and J. L. Martins, Phys. Rev. B **43**, 1993 (1991); L. Kleinman and D. M. Bylander, Phys. Rev. Lett. **48**, 1425 (1982).
[31] Y. Miyamoto *et al.*, Chem. Phys. Lett. **392**, 209 (2004).
[32] Y. Miyamoto, A. Rubio, and D. Tománek, Phys. Rev. Lett. **97**, 126104 (2006).
[33] T. Frauenheim *et al.*, J. Phys. Condens. Matter **14**, 3015 (2002).
[34] A. V. Krasheninnikov *et al.*, Chem. Phys. Lett. **418**, 132 (2006).
[35] A. V. Krasheninnikov *et al.*, Phys. Rev. B **72**, 125428 (2005).
[36] F. Banhart, J. X. Li, and A. V. Krasheninnikov, Phys. Rev. B **71**, 241408(R) (2005).